College of Pharmaceutical Sciences[1], Zhejiang University, Hangzhou, China; College of Medicine[2], Hangzhou Normal University, Hangzhou, China

Tofacitinib citrate-based liposomes for effective treatment of rheumatoid arthritis

Qiying Shen[1,2], Huan Shu[2], Xiaoling Xu[1], Gaofeng Shu[1], Yongzhong Du[1,*], Xiaoying Ying[1,*]

Received September 17, 2019, accepted December 30, 2019

**Corresponding authors: Yongzhong Du, Xiaoying Ying, College of Pharmaceutical Sciences, Zhejiang University, 866 Yuhangtang Road, Hangzhou 3110058, China*
duyongzhong@zju.edu.cn, yingxiaoying@zju.edu.cn

Pharmazie 75: 131-135 (2020) *doi: 10.1691/ph.2020.9154*

Low drug concentrations at interest sites and unwanted systemic side effects are major obstacles to effective therapy of rheumatoid arthritis (RA). With the aim of improving the efficacy of tofacitinib citrate (TOF), a liposomal system was developed for targeted delivery to inflamed joints, and this approach was validated in a RA rat model. TOF was effectively loaded into the liposomes (entrapment efficiency: 86.5±1.9%; drug loading: 2.3±0.05%) by a pH gradient method, and these molecules featured sustained drug release behaviour over 48 h. *In vitro* and *in vivo* studies showed that TOF loaded liposomes (TOFL) could be selectively taken up by inflamed cells and showed improved accumulation in arthritic paws, demonstrating the superior target ability to RA tissues. Moreover, compared to free TOF, TOFL significantly improved the therapeutic efficacy, reduced the inflammatory cytokine expression and lipid peroxidation in synovial cells in the joint tissue of RA rats. Overall, these results indicate that TOFL served as the useful nanocarriers for RA-targeted therapy.

1. Introduction

Rheumatoid arthritis (RA) is a complex autoimmune inflammatory disease inducing disability and work limitations (Hu et al. 2017; Smolen et al. 2018). Currently, a huge number of population (0.5-1%) worldwide is suffering from this disease (Hyndman 2016; McQueen 2017). Patients with RA are facing drug therapeutic regimens of high toxicity, limited effectivity and a significant risk of adverse effects, seriously affecting quality of life (Alam et al. 2017; Xu et al. 2018).

Tofacitinib is an oral Janus kinase 3 (JAK3) inhibitor for moderate to severe active rheumatoid arthritis with insufficient or intolerant response to MTX therapy (Zerbini and Lomonte 2012). As a new disease-modifying antirheumatic drug (DMARD), tofacitinib citrate (TOF) not only has a pain-relieving effect but also alters disease progression and articular damage (Song et al. 2014; Kawalec et al. 2018). However, tofacitinib citrate is commonly used for oral administration, which leads to a lack of specific targeting ability to the lesion site. Although patients are adhering well, the application of TOF is largely limited due to some critical issues, such as lower drug concentration at the sites of interest, unwanted systemic side effects, and poor therapeutic efficacy (Fleischmann et al. 2012; Wollenhaupt et al. 2014; Cohen et al. 2017). We postulate that nanocarrier drug delivery systems can enhance TOF therapy because of these systems can enable TOF to target RA sites effectively.

Nanomedicine, as potent therapeutics to improve pharmacokinetics and biodistribution of therapeutic agents, has been exploited widely over the past decades (Prasad et al. 2015; Shi et al. 2017). It is worth noting that the passive targeting strategy has been applied to improve delivery efficiency of drugs to inflamed tissue for effective treatment of RA by an extravasation through leaky vasculature and subsequent inflammatory cell-mediated sequestration (ELVIS) since RA is known as an angiogenesis-dependent disease (Wang et al. 2016; Alam et al. 2017; Heo et al. 2017). The ELVIS effect is analogous to the enhanced permeability and retention effect (EPR) in solid tumors (Wang et al. 2016; Shen and Qiu 2017). Some types of nanosized drug delivery systems (e.g., liposomes, micelles and nanoparticles) were employed to deliver anti-inflammatory drugs to the inflamed regions by a passive targeting strategy (Ulmansky et al. 2012; Wang et al. 2016; Feng and Chen 2018). As one of the best studied types of drug delivery systems, liposomes have been used clinically for anticancer therapy. Liposomes have attractive characteristics in delivering drugs to the RA site.

In this study, we hypothesized that the incorporation of TOF into nanoliposomes would enhance drug delivery to arthritic tissues. Nanoliposomes with a diameter of approximately 60 nm could achieve the efficient entrapment of TOF using a pH gradient method. We investigated the characteristics and *in vitro* activity of the nanoliposomes loaded with TOF (TOFL). The anti-inflammatory efficacy and toxicity of TOFL were also assessed by using an adjuvant-induced arthritis rat model. Our results highlight the targeting ability of TOFL to inflamed tissues when administered systemically, which is beneficial for safer and more effective treatment of RA.

2. Investigations, results and discussion

2.1. Characterization of the liposomes

TOFL was prepared using the pH gradient method. The physicochemical characterization of TOFL is exhibited in the Table. TOFL was uniformly distributed with a mean size of approximately 60 nm, which was measured by DLS (Fig. 1A). TEM confirmed that the TOFL had a uniform spherical shape (Fig. 1B).

Table: Physicochemical characterization of TOFL (mean ± SD, n = 3)

Size (nm)	EE (%)	DL (%)	PDI	Zeta potential (mV)
59.63 ± 4.05	86.46 ± 1.89	2.31 ± 0.05	0.23 ± 0.03	-2.27 ± 0.35

In order to evaluate the stability of liposomes, TOFL solutions were stored for 48 h at 25 °C. As exhibited in Fig. 1C, PDI of TOFL did not change significantly over 48 h, and size increased slightly over the same period, indicating there was no aggregation or precipitation in the TOFL solution. Good stability lays the foundation for the application of the TOFL in 10% serum-containing PBS.

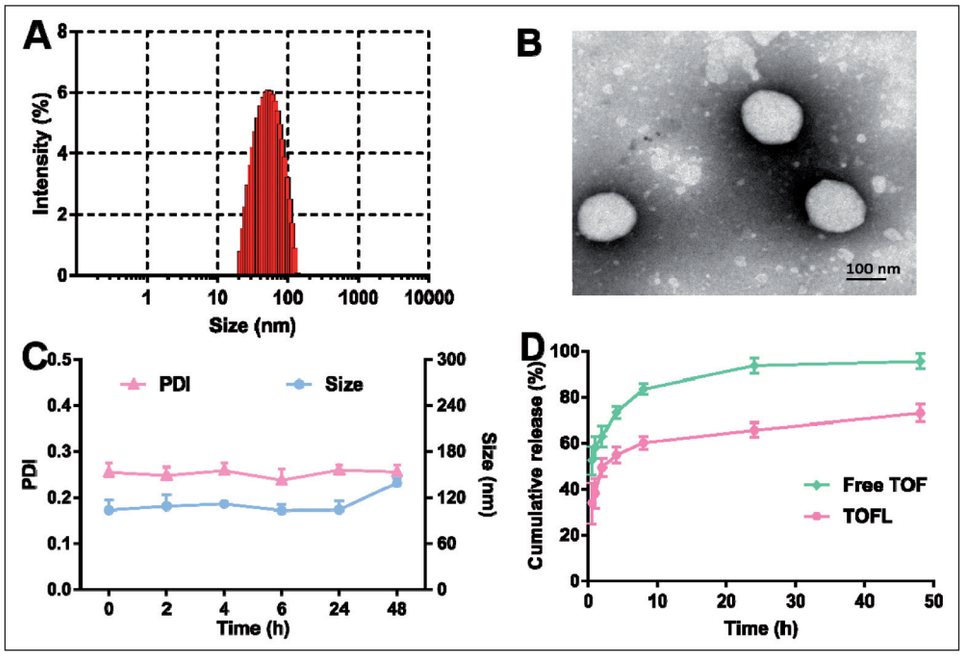

Fig. 1: Physicochemical characterization of TOFL. (A) Size distribution and (B) TEM images. Scale bar, 100 nm. (C) Stability of TOFL at 25 °C for 48 h. (D) *In vitro* release profiles of free TOF and TOFL at 37 °C in pH 7.4 PBS. The results represent as the mean values ± SD (n = 3).

The release profile of TOFL was examined in PBS (pH 7.4) at 37 °C, in which free TOF was studied as a control (Fig. 1D). It was found that free TOF was rapidly released, with over 80% of drug was released within the first 10 h. In contrast, the percentage of TOF released from TOFL was less than 60% even after 48 h, suggesting that TOFL had a relatively low leakage under the test conditions.

2.2. Viability of the cell culture

The cell viabilities of blank-L, free TOF and TOFL towards HUVECs were examined by MTT assay. Apparently, blank-L has extremely low cytotoxicity towards HUVECs, as over 80% of cells were still survived at the highest concentration of 1000 μg/mL (Fig. 2A). As shown in Fig. 2B, the cell viabilities were >80% when the cells incubated with free TOF or TOFL at the highest

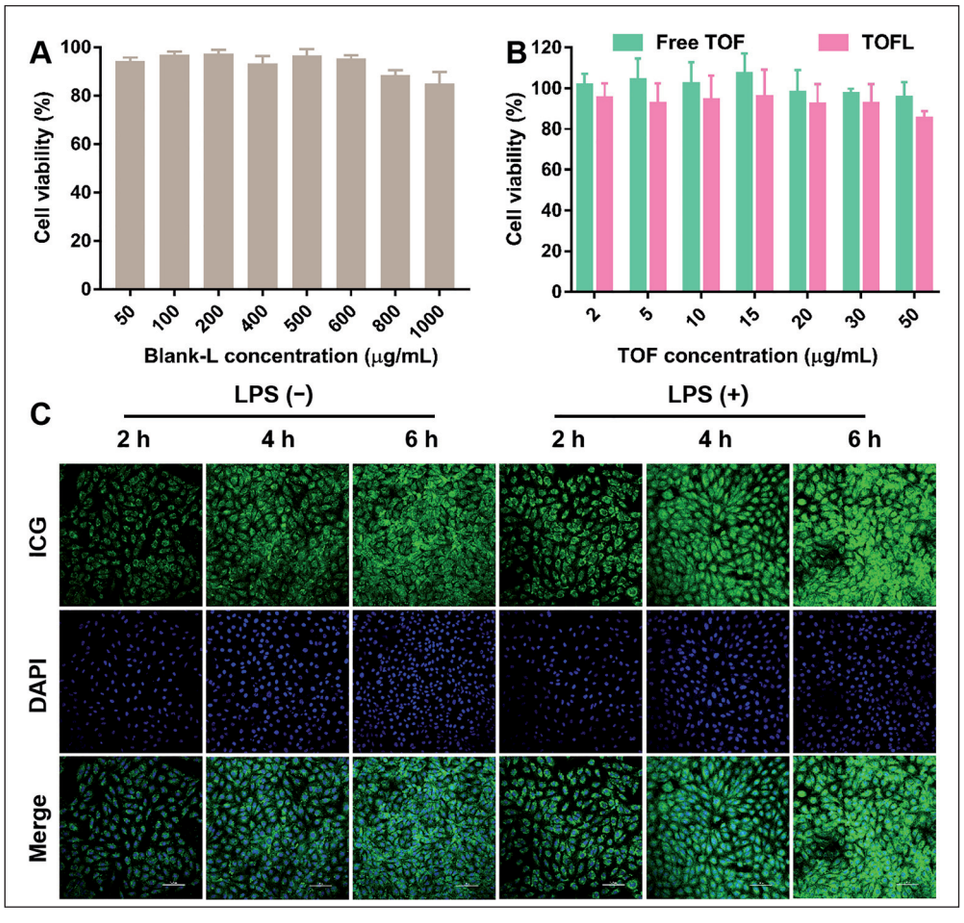

Fig. 2: Viability of HUVEC cultures after exposure to **(A)** blank-L, **(B)** Free TOF and TOFL. Viability was calculated relative to that of untreated cells (100%). The data shown are the means ± SD (n=3). **(C)** Confocal microscope images showing the uptake of ICGL with nonactivated or LPS-activated HUVECs at 2 h, 4 h, and 6 h.

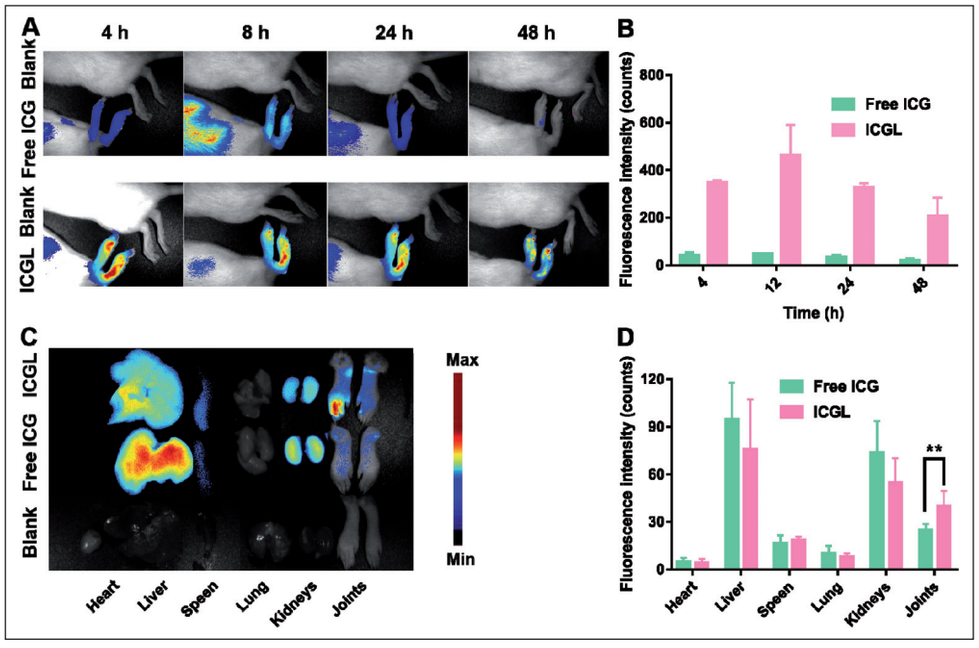

Fig. 3: Biodistribution of ICGL in RA rats. (A) Real-time fluorescence imaging and (B) Quantification of fluorescence intensity of rats after intravenous injection of free ICG or ICGL at 4 h, 8 h, 24 h and 48 h. (C) Ex vivo images of dissected tissues. Untreated rats served as the negative control. (D) Quantification of fluorescence intensity in each organ. Data are shown as the means ± SD (n= 3). **P < 0.01, ***P < 0.001.

concentration of 50 μg/mL, indicating that TOF and TOFL was little toxic towards HUVECs.

2.3. Intracellular accumulation of liposomes by HUVECs

To evaluate the cellular uptake of the liposomes, HUVECs with or without LPS activation were treated with ICG-loaded liposomes (ICGL). As shown in Fig. 2C, the green fluorescence notably intensified as the incubation time was increased from 2 to 6 h. This result suggested that liposomes could be effectively internalized by HUVECs in a time-dependent manner. LPS-activated HUVECs showed a significantly stronger fluorescence signal than nonactivated ones. Apparently, LPS activation further enhanced the uptake of liposomes. The reason for this phenomenon was that LPS improves the cell permeability of membrane, which may facilitate the Toll-like receptor-mediated endocytosis of the liposomes (Gao et al. 2006).

2.4. Biodistribution analyses in RA rats

To investigate the *in vivo* biodistribution and RA-targeting characteristics of the liposomes, ICG-loaded liposomes were injected intravenously into RA rats. Time-dependent images of the whole hind legs were evaluated over time up to 48 h. The nearing fared (NIRF) images showed arthritic paws of rats treated with ICGL had significantly higher fluorescence intensity at 4 h, 8 h, 24 h and 48 h, indicating rapid distribution, relatively long persistence in circulation, and the high RA-targeting ability of the liposomes, while the free ICG was rapidly excreted and could not accumulate and stay in the hindlimbs. (Fig. 3A, B).

The highest fluorescence in rats treated with ICGL was observed in the liver and limbs according to the *ex vivo* imaging of different organs and tissues (Fig. 3C, D). In contrast, as for the free ICG treated rats, the highest fluorescence was observed in the liver and kidney. These results suggested that liposomes were selectively accumulated in arthritic joints. The improved selective accumulation in arthritic joints by formulating ICG into nanomedicines should be attributed to passive targeting achieved by ELVIS effect, a unique feature that allows macromolecules or nanocarriers to preferentially accumulate in inflamed tissue (Wang and Sun 2017; Hou et al. 2018).

2.5. In vivo therapeutic efficiency

After initial drug administration, body weight, paw thickness and arthritic joint scores of rats were measured every day for nearly two weeks. In all of the evaluated groups, no significant body weight changes were observed (Fig. 4A). The forelimb and hindlimb joints of the RA rats were assigned to arthritic scores on a scale ranging from 0 to 4 to reflect the severity of inflammation and swelling (Song et al. 2015). The PBS-treated group exhibited serious inflammation in the joints, as reflected by the rapid increase in paw thickness. Compared with the PBS-treated rats, the paw thickness of both free TOF- and TOFL-treated rats were associated with slower disease progression, TOFL-treated group slowing progression to a greater extent (Fig. 4B). Consistent with the inflammation results, the arthritic joint scores were the highest in the PBS group, followed by the free TOF group and finally by the TOFL group (Fig. 4C). These data clearly showed that the TOFL significantly relieved the paw thickness and arthritic joint scores, which might result from the release of TOF from the liposomes after passively targeting to the RA site.

2.6. Pro-inflammatory cytokine expression joint tissue after therapy

JAK3 mainly mediates the synthesis of interleukin (IL), a kind of cytokines, of which the pro-inflammatory ones play an important role in the cartilage tissue damage and repair, which means that JAK3 plays a pivotal role in the pathogenesis of RA (Ghoreschi et al. 2009; Meyer et al. 2010). Tofacitinib, as a kind of JAK3 inhibitor, can block the phosphatization of JAK3, further lead to the inhibition of synthesis of downstream pro-inflammatory cytokines (Zerbini and Lomonte 2012). Two of the most important pro-inflammatory cytokines are TNF-α and IL-6, which contribute to the pathogenesis and progression of RA. (Feldmann and Maini 2008; Lee et al. 2014; Kim et al. 2015). In fact, their levels in joint tissue can be used as surrogate markers of therapeutic efficacy for anti-arthritis drugs. We measured their levels in RA rats treated with PBS, free TOF, or TOFL as another index of therapeutic efficacy. RA rats treated with PBS showed significantly upregulated expression levels of TNF-α and IL-6 (Fig. 4D, E). However, these levels were not significantly affected by treatment with free TOF, and relatively lower levels were observed after treatment with TOFL. These results indicated that TOFL had greater anti-inflammatory activity than free TOF or PBS.

2.7. Histopathology of the ankle joints after therapy

The histological analysis of the knee joints was performed in comparison to normal Wistar rats. The knee joints of the PBS-,

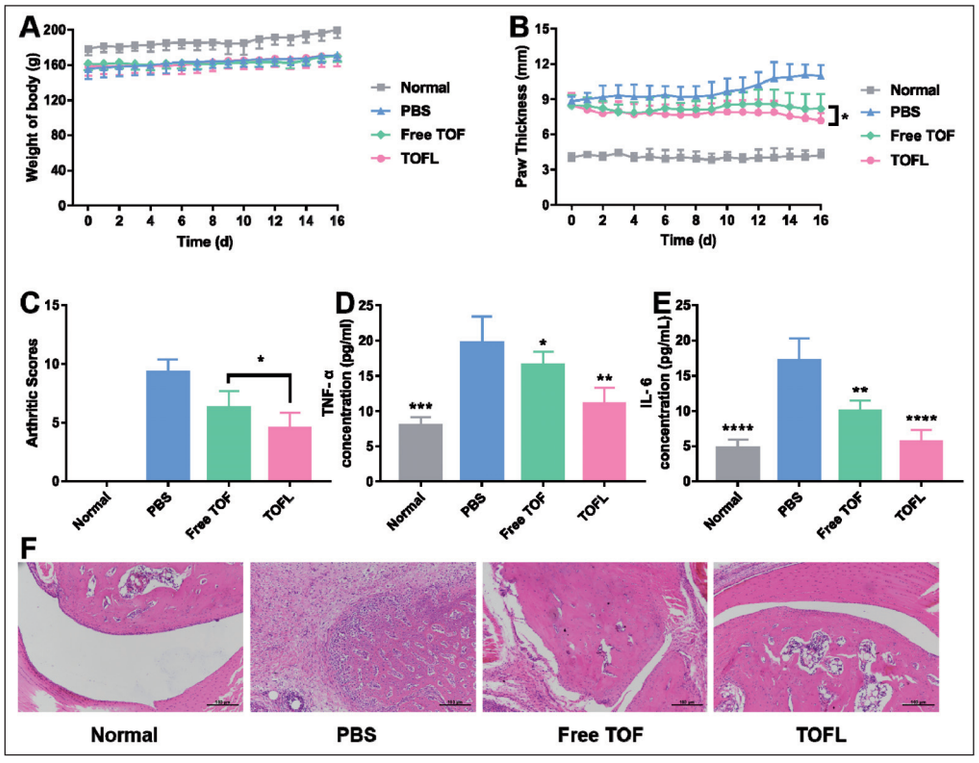

Fig. 4: Arthritis induction in rats and assessment of therapeutic effects based on (A) body weight changes, (B) hind paw thickness, and (C) joint scores (n = 7). Expression of pro-inflammatory cytokines (D) TNF-α and (E) IL-6 in joint tissue of arthritic rats treated with PBS, free TOF, or TOFL as measured by ELISA. The results are shown as the means ± SD (n = 5). *P< 0.05, **P< 0.01, ***P< 0.001, ****P< 0.0001. (F) Histopathology in ankle joints was identified using haematoxylin-eosin staining.

free TOF-, and TOFL-treated rats were assessed by H&E to further evaluate the therapeutic efficacy (Fig. 4F). Normal rats without RA induction showed no signs of inflammation or destruction of cartilage and bone. The interface between cartilage and bone in the tissues were clearly distinguished according to their morphologies. However, RA model rats treated with PBS showed severe inflammatory cell infiltration, lipid peroxidation in synovial cells, extensive synovitis and pannus formation, articular cartilage destruction, and bone destruction. On the other hand, the knee joints from free TOF-treated rats exhibited slightly less signs of inflammation. However, compared to the PBS- and free TOF-treated rats, the knee joints from TOFL-treated groups exhibited a clear interface and showed significant reduction of pathologic features, including synovial hyperplasia, lipid peroxidation in synovial cells, pannus formation, and bone erosion, which were consistent with the therapeutic efficiency of TOFL.

2.8. Conclusion

In conclusion, we successfully constructed liposomal systems for loading the small water-soluble drug, tofacitinib citrate, with efficient entrapment, and its potential to be a targeted nanocarrier for RA was investigated. The prepared TOFL were readily taken up by activated HUVECs. Due to passive targeting mechanisms, systemically administered TOFL accumulated selectively in the inflamed tissue of RA. Moreover, compared to free TOF, TOFL significantly promoted the alleviation of the clinical symptoms in joint tissue of RA rats. Overall, these results indicated that TOFL is beneficial for achieving enhanced efficacy in RA.

3. Experimental

3.1. Materials, cell culture, and animal model

Cholesterol (Chol) was purchased from Tokyo Chemical Industry (Tokyo, Japan). Soybean phosphatidylcholine (SPC) was obtained from Lipoid (GmbH, Ludwigshafen, Germany). Indocyanine green (ICG) was supplied by TCI (Tokyo, Japan). Tofacitinib citrate (TOF) was supplied by Boc Chemical Co., Ltd. (Shanghai, China). Lipopolysaccharide (LPS), dimethyl sulfoxide (DMSO) and 3-(4,5-dimethyl-2-thiazolyl)-2,5-diphenyltetrazolium bromide (MTT) were acquired from Sigma Aldrich (Saint Louis, MO, USA). Rat TNF-alpha and Rat IL-6 ELISA kits were obtained from Boster Biological Technology Co., Ltd. (Wuhan, China). Disodium hydrogen phosphate dodecahydrate and potassium phosphate monobasic were purchased from Sinopharm Chemical Reagent Co., Ltd. (Shanghai, China). All other chemicals were of a commercially available grade.

The human umbilical vein endothelial cell (HUVEC) line was obtained from KeyGEN BioTech (Nanjing, China), which was grown in Dulbecco's modified Eagle's medium (DMEM, Genom Co., Ltd., Hangzhou, China) containing 10% foetal bovine serum (FBS), 100 U/mL penicillin, and 100 U/mL streptomycin and incubated at 37 °C in a humidified atmosphere of 5% CO_2.

Wistar rats aged 6-8 weeks (160-180 g) were purchased from the Zhejiang Academy of Medical Sciences (Hangzhou, China). Animal experiments were carried out in strict accordance with review and approval by the Animal Ethical and Experimental Committee of Zhejiang University.

3.2. Formulation preparation

Tofacitinib citrate liposomes (TOFL) were prepared by two steps: blank liposomes (blank-L) and drug-loaded liposomes, as described previously (Shen and Qiu 2017). First, the blank liposomes were prepared by a thin film hydration method. Chol (50 mg) and SPC (100 mg) were dissolved in ethanol, and the mixture was dried under reduced pressure at 50 °C with a rotary evaporator for approximately 30 min and hydrated with 2 mL of $C_6H_8O_7$-$C_7H_5O_3Na$ (pH 3.6) as an internal buffer in a vortex mixer. The liposome dispersions were ultrasonicated for 20 min in ice bath and then filtered through a 0.22 μm filter membrane to homogenize the size of the blank liposomes. Second, TOF was loaded into liposomes by a pH gradient method. The external pH of the liposomes was adjusted to pH 8 by Na_2CO_3 and then these liposomes were mixed with TOF (4 mg) solution. This mixture was finally incubated at 60 °C for 10 min by occasional shaking, and the free TOF was removed by ultrafiltration.

3.3. Characterization of TOFL

The size distribution, polydispersity (PDI) and zeta potential of TOFL were analysed by dynamic light scattering (DLS) (Litesizer 500, Anton Paar, Graz, Austria). The morphology and size were also observed using transmission electron microscopy (TEM) (JEM-1230, JEOL Ltd., Tokyo, Japan).

Entrapment efficiency (EE) and drug loading (DL) were measured using an ultrafiltration tube with a molecular weight cut-off of 10 kDa (Millipore, Massachusetts, USA). Unencapsulated TOF in the substrate was measured by high-performance liquid chromatography (HPLC) (1200, Agilent, USA). Total TOF was also determined after destruction by methanol. EE and DL were calculated.

As for the stability assay, TOFL were stored for 48 h in 10% serum-containing medium at 25 °C. The protocol used was similar to the previous description with a few modifications (Wang et al. 2016). The size and PDI were measured at indicated time points.

To investigate the *in vitro* release of TOF from TOFL, a dialysis bag method was carried out (Shen and Qiu 2017). In brief, 0.5 ml of newly prepared TOFL was dispersed in the dialysis and incubated at 37 °C in 40 ml PBS (pH 7.4) with constant shaking, and the concentration of TOF at various time points was quantified by HPLC.

3.4. Viability of cell culture

MTT assays were used to detect the viability of cells treated with blank-L, free TOF, and TOFL. HUVECs were seeded onto a 96-well plate at 5.0×10^3 cells per well and incubated overnight at 37 °C in a humidified atmosphere with 5% CO_2. Then, the cells were treated for 48 h with blank-L, free TOF, or TOFL at various doses. Finally, the MTT assay was applied to quantify the cell viability.

3.5. Intracellular accumulation of liposomes by HUVECs

The detection of intracellular accumulation of liposomes was performed as described previously (Alam et al, 2017; Shen and Qiu 2017). Briefly, HUVECs were cultured on 6-well plates (1×10^5 cells per well) in the absence or presence of lipopolysaccharide (LPS, 50 ng/mL) for 24 h. For detection by flow cytometry, indocyanine green (ICG) was incorporated into the liposomes instead of TOF. The fluorescent dye ICG-loaded liposomes (ICGL) were added to the cultures and then incubated at 37 °C for various times. Following this incubation, the cells were digested, collected, and washed three times with cold PBS. Finally, the cells were resuspended in PBS for flow cytometric analysis.

For confocal laser microscopy, HUVECs were seeded onto glass coverslips in 6-well plates. After ICGL (at a final ICG concentration of 25 μg/mL) treatment at 37 °C for various times, the cells were washed three times with cold PBS. Then, the cell nuclei were stained with Hoechst 33258 for 15 min and fixed with 4% (v/v) paraformaldehyde solution for 30 min at 37 °C. Confocal microscopy analysis was performed by laser-scanning confocal microscopy (Nikon A1R, Tokyo, Japan).

3.6. Biodistribution analyses on RA rats

The fluorescent dye ICG was loaded into the liposomes by thin film hydration method to investigate the passive targeting ability of the liposomes. Female Waster rats (aged 6-8 weeks and weighing 150-170 g) were purchased from the Zhejiang Academy of Medical Sciences (Hangzhou, China) to establish the RA model as previously described (Fu et al. 2015). In this experiment, free ICG or ICGL (ICG concentration 1 mg/kg) were injected into the tail veins of RA rats at a dose of 1 mg/kg (Song et al. 2015; Xu et al. 2018). The *in vivo* biodistribution and RA-targeting efficacy were assessed using the Maestro In Vivo Imaging System (CRi, Inc., MA, USA), and images were taken at 4, 8, 24, and 48 h after administration to evaluate rapid distribution and the long-term effectiveness of maintenance of liposomes. Then, the RA rats were sacrificed, and the organs were dissected. Ex vivo fluorescence images were obtained with this imaging system.

3.7. In vivo therapeutic efficiency

Treatment began from day 7 after arthritis induction and lasted until day 23. Five healthy Waster rats without any treatment were served as a normal group. RA rats were divided into three groups and treated by intravenous injection: PBS (control group, n = 7), free TOF (0.2 mg/kg, n = 7), and TOFL (0.2 mg/kg, n = 7). Each treatment was injected daily, and paw thickness was determined by callipers, and joint scores were assessed, which were summed for each mouse with a maximum possible score of 16 (Wang et al. 2016).

3.8. Pro-inflammatory cytokine expression in joint tissue after therapy

After about two weeks of therapy, all animals were euthanized, and the joint tissues were dissected. According to the manufacturer's instructions, the levels of the pro-inflammatory cytokines, TNF-α and IL-6, in the joints were quantitated by ELISA kits.

3.9. Histopathology of ankle joints after therapy

For histological analysis, the dissected joints were fixed in 4% paraformaldehyde for 48 h and decalcified completely by 15% neutral EDTA solution. The decalcified tissue was embedded in paraffin and cut into 5 mm-thick sections, which were stained with H&E.

3.10. Statistical analysis

The results were reported as the means±standard deviation (SD), analysed and graphed using GraphPad Prism 7.0 (GraphPad Software, La Jolla, CA, USA). One-way or two-way analysis of variance (ANOVA) was used to assess differences and correlations for significance.

Acknowledgements: This study was supported by the National Nature Science Foundation of China (81771962), the Public Welfare Project of Zhejiang Province (LGF20H300005), the Scientific Research Project of Zhejiang Provincial Department of Education (Y201942272).

Conflict of interest: The authors declare no conflict of interest.

References

Alam MM, Han HS, Sung SJ, Kang JH, Sa KH, Faruque HA, Hong J, Nam EJ, Kim IS, Park JH, Kang YM (2017) Endogenous inspired biomineral-installed hyaluronan nanoparticles as pH-responsive carrier of methotrexate for rheumatoid arthritis. J Control Release 252: 62–72.

Cohen SB, Tanaka Y, Mariette X, Curtis JR, Lee EB, Nash P, Winthrop KL, Charles-Schoeman C, Thirunavukkarasu K, DeMasi R, Geier J, Kwok K, Wang L, Riese R, Wollenhaupt J (2017) Long-term safety of tofacitinib for the treatment of rheumatoid arthritis up to 8.5 years: integrated analysis of data from the global clinical trials. Ann Rheum Dis 76: 1253–1262.

Feldmann M, Maini SR (2008) Role of cytokines in rheumatoid arthritis: an education in pathophysiology and therapeutics. Immunol Rev 223: 7–19.

Feng X, Chen Y (2018) Drug delivery targets and systems for targeted treatment of rheumatoid arthritis. J Drug Target 26: 845–857.

Fleischmann R, Kremer J, Cush J, Schulze-Koops H, Connell CA, Bradley JD, Gruben D, Wallenstein GV, Zwillich SH (2012) Placebo-controlled trial of tofacitinib monotherapy in rheumatoid arthritis. N Engl J Med 367: 495–507.

Fu J, Lv XY, Qiu LY (2015) Thermo-responsive triblock copolymer micelles containing PEG6000 for either water-soluble or water-insoluble drug sustained release and treatment. RSC Adv 5: 37451–37461.

Gao J, Zhou WX, Zhou LJ, Zeng BX, Yao SL, Liu D, Chen ZQ (2006) Protective effects of propofol on lipopolysaccharide activated endothelial cell barrier dysfunction. Inflamm Res 55: 385–392.

Ghoreschi K , Laurence A, O' Shea JJ (2009) Janus kinases in immune cell signaling. Immunol Rev 228: 273–287.

Heo R, You DG, Um W, Choi KY, Jeon S, Jong-Sung P, Choi Y, Kwon S, Kim K, Kwon IC, Dong-Gyu J, Kang YM, Park JH (2017) Dextran sulfate nanoparticles as a theranostic nanomedicine for rheumatoid arthritis. Biomaterials 131: 15–26.

Hu H, Luan L, Yang KQ, Li SC (2017) Psychometric validation of Chinese Health Assessment Questionnaire for use in rheumatoid arthritis patients in China. Int J Rheum Dis 20: 1987–1992.

Hyndman IJ (2016) Rheumatoid arthritis: past, present and future approaches to treating the disease. Int J Rheum Dis 19: 325–328.

Kawalec P, Śladowska K, Malinowska-Lipień I, Brzostek T, Kozka M (2018) European perspective on the management of rheumatoid arthritis: clinical utility of tofacitinib. Ther Clin Risk Manag 14: 15–29.

Kim GW, Lee NR, Pi RH, Lim YS, Lee YM, Lee JM, Jeong HS, Chung SH (2015) IL-6 inhibitors for treatment of rheumatoid arthritis: past, present, and future. Arch Pharm Res 38: 575–584.

Lee H, Lee MY, Bhang SH, Byung-Soo K, Kim YS, Ju JH, Kim KS, Hahn SK (2014) Hyaluronate-gold nanoparticle/ tocilizumab complex for the treatment of rheumatoid arthritis. Acs Nano 8: 4790–4798.

McQueen FM (2017) Rheumatology around the world: perspectives from Australia and New Zealand. Arthritis Res Ther 19: 1–3.

Meyer DM, Jesson MI, Li X, Elrick MM, Funckes-Shippy CL, Warner JD, Gross CJ , Dowty ME, Ramaiah SK, Hirsch JL, Saabye MJ, Barks JL, Kishore N, Morris DL (2010) Anti-inflammatory activity and neutrophil reductions mediated by the JAK1/JAK3 inhibitor, CP-690, 550, in rat adjuvant-induced arthritis. J Inflamm 7: 41.

Prasad LK, O'Mary H, Cui Z (2015) Nanomedicine delivers promising treatments for rheumatoid arthritis. Nat Rev Drug Discov 10: 2063–2074.

Shen QY, Qiu LY (2017) Reversal of P-glycoprotein-mediated multidrug resistance by doxorubicin and quinine co-loaded liposomes in tumor cells. J Liposome Res 27: 293–301.

Shi JJ, Kantoff PW, Wooster R, Farokhzad OC (2017) Cancer nanomedicine: progress, challenges and opportunities. Nat Rev Cancer 17: 20–37.

Smolen JS, Aletaha D, Barton A, Burmester GR, Emery P, Firestein GS, Kavanaugh A, Mclnnes LB, Solomon DH, Strand V, Yamamoto K (2018) Rheumatoid arthritis. Nat Rev Dis Primers 4: 18001.

Song GG, Bae SC, Lee YH (2014) Efficacy and safety of tofacitinib for active rheumatoid arthritis with an inadequate response to methotrexate or disease-modifying antirheumatic drugs: a meta-analysis of randomized controlled trials. Korean J Intern Med 29: 656–663.

Song HP, Li X, Yu R, Zeng G, Yuan ZY, Wang W, Huang HY, Cai X (2015) Phenotypic characterization of type II collagen-induced arthritis in Wistar rats. Exp Ther Med 10: 1483–1488.

Ulmansky R, Turjeman K, Baru M, Katzavian G, Harel M, Sigal A, Naparstek Y, Barenholz Y (2012) Glucocorticoids in nano-liposomes administered intravenously and subcutaneously to adjuvant arthritis rats are superior to the free drugs in suppressing arthritis and inflammatory cytokines. J Control Release 160: 299–305.

Wang Q, Jiang JY, Chen WF, Jiang H, Zhang ZR, Sun X (2016) Targeted delivery of low-dose dexamethasone using PCL-PEG micelles for effective treatment of rheumatoid arthritis. J Control Release 230: 64–72.

Wang Q, Sun X (2017) Recent advances in nanomedicines for the treatment of rheumatoid arthritis. Biomater Sci 5: 1407–1420.

Wollenhaupt J, Silverfield J, Lee EB, Curtis JR, Wood SP, Soma K, Nduaka CI, Benda B, Gruben D, Nakamura H, Komuro Y, Zwillich SH, Wang L, Riese RJ (2014) Safety and efficacy of tofacitinib, an oral janus kinase inhibitor, for the treatment of rheumatoid arthritis in open-label, longterm extension studies. J Rheumatol 41: 837–852.

Xu XL, Li WS, Wang XJ, Du YL, Kang XQ, Hu JB, Li SJ, Ying XY, You J, Du YZ (2018) Endogenous sialic acid-engineered micelles: a multifunctional platform for on-demand methotrexate delivery and bone repair of rheumatoid arthritis. Nanoscale 10: 2926–2935.

Zerbini CA, Lomonte AB (2012) Tofacitinib for the treatment of rheumatoid arthritis. Expert Rev Clin Immunol 8: 319–331.

Zhou M, Hou J, Zhong Z, Hao N, Lin Y, Li C (2018) Targeted delivery of hyaluronic acid-coated solid lipid nanoparticles for rheumatoid arthritis therapy. Drug Deliv 25: 716–722.